

## $\beta$ -Cyclodextrin Polymers with Different Cross-Linkers and Ion-Exchange Resins Exhibit Variable Adsorption of Anionic, Zwitterionic, and Nonionic PFASs

Casey Ching, Max J. Klemes, Brittany Trang, William R. Dichtel,\* and Damian E. Helbling\*


 Cite This: *Environ. Sci. Technol.* 2020, 54, 12693–12702


Read Online

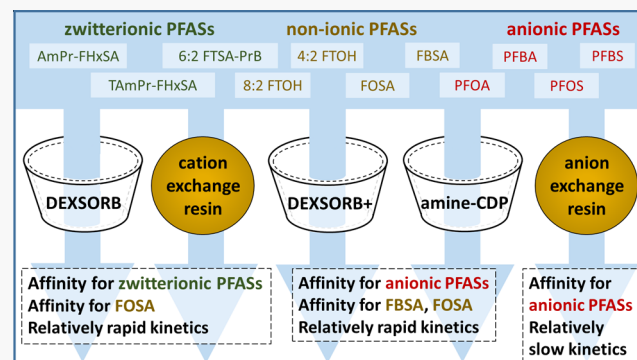
ACCESS |

Metrics &amp; More

Article Recommendations

Supporting Information

**ABSTRACT:** Per- and polyfluoroalkyl substances (PFASs) occur in groundwater as mixtures of anionic, cationic, zwitterionic, and nonionic species, although few remediation technologies have been evaluated to assess the removal of different types of PFASs. In this study, we evaluated the performance of three  $\beta$ -cyclodextrin polymers (CDPs), an anion-exchange (AE) resin, and a cation-exchange (CE) resin for the removal of anionic, zwitterionic, and nonionic PFASs from water. We found that a CDP with a negative surface charge rapidly removes all zwitterionic PFASs with  $\log K_D$  values ranging between 2.4 and 3.1, and the CE resin rapidly removes two zwitterionic PFASs with  $\log K_D$  values of 1.8 and 1.9. The CDPs with a positive surface charge rapidly remove all anionic PFASs with  $\log K_D$  values between 2.7 and 4.1, and the AE resin removes all anionic PFASs relatively slowly with  $\log K_D$  values between 2.0 and 2.3. All adsorbents exhibited variable removal of the nonionic PFASs and some adsorption inhibition at higher pH values and in the presence of groundwater matrix constituents. Our findings provide insight into how adsorbents can be combined to remediate groundwater contaminated with complex mixtures of different types of PFASs.



### INTRODUCTION

There is increasing concern over the occurrence of per- and polyfluoroalkyl substances (PFASs) in groundwater because of their persistence and associated health effects.<sup>1–4</sup> Although much attention has focused on the anionic perfluoroalkyl acids, including perfluorooctanoic acid (PFOA) and perfluorooctanesulfonic acid (PFOS), recent studies demonstrate that groundwater can contain PFASs from a variety of other classes, including cationic, zwitterionic, and nonionic PFASs.<sup>5–12</sup> Although significantly less is known about the environmental behavior and toxicity of these other classes of PFASs,<sup>7</sup> many exhibit similar levels of persistence and may accumulate in biological tissues in similar ways.<sup>2,13</sup> Additionally, some zwitterionic and cationic PFASs can be transformed into perfluoroalkyl acids in natural and engineered systems.<sup>12,14–16</sup> Therefore, remediation technologies should be evaluated for their potential to remove a variety of PFAS classes.

Adsorption technologies have emerged as one of the most promising techniques for the remediation of PFAS-contaminated groundwater.<sup>17–20</sup> Granular activated carbon (GAC) and ion-exchange resins are widely studied adsorbents that are commonly implemented in full-scale adsorption processes.<sup>21–23</sup> GAC is a nonselective adsorbent that exhibits moderate affinity for long-chain perfluoroalkyl acids but

performs poorly for short-chain perfluoroalkyl acids.<sup>17,24</sup> Furthermore, GAC exhibits slow, diffusion-limited adsorption kinetics<sup>25,26</sup> and is readily fouled by matrix constituents including inorganic ions and natural organic matter (NOM).<sup>27</sup> These deficiencies have motivated studies focused on anion-exchange (AE) resins as an alternative adsorbent for the remediation of PFAS-contaminated groundwater.<sup>28,29</sup> AE resins exhibit higher affinity for short-chain perfluoroalkyl acids,<sup>17,24</sup> higher adsorption capacity,<sup>17,24</sup> and faster adsorption kinetics<sup>28</sup> when compared to GAC, although their performance can likewise be inhibited by the presence of NOM or other inorganic ions,<sup>21,30–32</sup> and AE resins can exhibit preferential adsorption of perfluorosulfonic acids over perfluorocarboxylic acids.<sup>33</sup> To the best of our knowledge, no published study has explored the use of cation-exchange (CE) resins for remediation of PFAS-contaminated groundwater, although CE resins may exhibit greater affinity for zwitterionic and cationic PFASs. Although ion exchange is the predominant

Received: June 19, 2020

Revised: September 10, 2020

Accepted: September 14, 2020

Published: September 14, 2020



mechanism determining adsorbate uptake on ion-exchange resins, other known mechanisms (e.g., electrostatic interactions, hydrophobic interactions, and micelle or hemimicelle formation) may contribute to the removal of nonanionic PFASs.<sup>31–33</sup> To our knowledge, no studies have evaluated the removal of nonanionic PFASs using ion-exchange resins.

Cyclodextrin polymers (CDPs) are a class of emerging adsorbents that rapidly remove a variety of chemicals from water.<sup>34–36</sup> Cyclodextrins are macrocycles of glucose that can bind organic molecules within their interior cavity by means of hydrophobic interactions.<sup>37</sup> The most promising CDPs for water remediation contain  $\beta$ -cyclodextrin cross-linked with a rigid aromatic group that is functionalized to impart a surface charge to enhance their affinity for charged adsorbates.<sup>38,39</sup> For example, a tetrafluoroterephthalonitrile (TFN)-cross-linked CDP with a negative surface charge exhibits rapid uptake and high affinity for a variety of nonionic and cationic micropollutants,<sup>35,40,41</sup> whereas a postsynthetically modified derivative of the TFN-CDP with a positive surface charge exhibits rapid uptake and high affinity for nonionic and anionic micropollutants.<sup>39</sup> The unique binding mechanism of CDPs can limit adsorption inhibition by large-molecular-weight NOM and other matrix constituents, which either cannot access or do not bind to the interior cavity of the cyclodextrins,<sup>35,42,43</sup> making CDPs promising adsorbents for environmental remediation. Others have also demonstrated that the interior cavity of  $\beta$ -cyclodextrin is an excellent receptor for linear perfluoroalkyl chains.<sup>44–47</sup> We recently demonstrated that CDPs with a positive surface charge exhibit rapid adsorption kinetics and nearly complete removal of anionic PFASs from water.<sup>39,43</sup> However, no previous study has explored the use of different types of CDPs for the removal of cationic, zwitterionic, or nonionic PFASs under variable environmental conditions.

The primary objective of this study was to evaluate the performance of CDPs with different cross-linkers for the removal of different classes of PFASs from water. We selected three CDPs that exhibit different surface charges and evaluated their potential to remove a set of 11 PFASs from water. The PFASs included four anionic PFASs, three zwitterionic PFASs, and four nonionic PFASs. We simultaneously evaluated the performances of an AE resin and a CE resin to evaluate the breadth of their PFAS removal potential. For each adsorbent, we measured (i) adsorption kinetics for the 11 PFASs; (ii) adsorbent affinity for the 11 PFASs; and (iii) adsorption inhibition across a gradient of pH values in the presence and absence of groundwater matrix constituents. We found that each adsorbent exhibits variable adsorption kinetics and variable adsorption affinity for anionic, zwitterionic, and nonionic PFASs while also exhibiting some adsorption inhibition at higher pH values and in the presence of groundwater matrix constituents.

## MATERIALS AND METHODS

**Chemicals and Reagents.** Eleven PFASs were selected to represent a set of anionic, zwitterionic, and putatively nonionic PFASs at circumneutral pH; we note that authentic standards for exclusively cationic PFASs were not commercially available at the time of the study. Four anionic PFASs including perfluorobutanoic acid (PFBA), perfluorobutanesulfonic acid (PFBS), PFOA, and PFOS were selected to benchmark our data with other studies and to represent varying carbon chain lengths and anionic head groups. The three zwitterionic PFASs

included *N*-dimethylammoniopropyl perfluorohexane sulfonamide (AmPr-FHxSA), *N*-trimethylammoniopropyl perfluorohexane sulfonamide (TAmPr-FHxSA), and 6:2 fluorotelomer sulfonamidopropyl betaine (6:2 FTSA-PrB, previously identified as 6:2 FTAB in the literature). All three of the zwitterionic PFASs contain a six-carbon perfluorinated chain, have been detected in PFAS-contaminated groundwater,<sup>6,7,48</sup> and are expected to be zwitterions at circumneutral pH, although some fraction of each will be cationic at lower pH values.<sup>49–51</sup> The four putatively nonionic PFASs<sup>49,51,52</sup> included perfluoro-1-butanesulfonamide (FBSA), perfluoro-1-octanesulfonamide (FOSA), 2-perfluorobutyl ethanol (4:2 FTOH), and 2-perfluoroctyl ethanol (8:2 FTOH). We note that  $pK_a$  estimates for FBSA and FOSA vary greatly and one estimate suggests that both would be predominantly anionic at circumneutral pH;<sup>49,52</sup> nevertheless, some fraction of each will be nonionic at lower pH values. Authentic standards of PFBA (Sigma-Aldrich), PFOA (Sigma-Aldrich), PFBS (TCI American), and PFOS (Santa Cruz Biotechnology) were purchased as solids and prepared at a concentration of 1 g L<sup>−1</sup> in 100% LCMS-grade methanol (MilliporeSigma). Authentic standards of 4:2 FTOH, 8:2 FTOH, AmPr-FHxSA, TAmPr-FHxSA, and 6:2 FTSA-PrB were purchased from Wellington Laboratories as 50 mg L<sup>−1</sup> in 100% methanol and were used as received. Authentic standards of FBSA and FOSA were purchased from Wellington Laboratories as 50 mg L<sup>−1</sup> in 100% isopropanol and were used as received. A 1 mg L<sup>−1</sup> stock mixture solution containing the 11 PFASs was prepared in nanopure water with 2% LCMS-grade methanol (MilliporeSigma). PFAS suppliers, structures, and estimated  $pK_a$  values of each PFAS are provided in Table S1 of the Supporting Information.

**Adsorbents.** Five adsorbents were selected for this study. DEXSORB and DEXSORB+ (Cyclopure Inc., Encinitas, CA) are commercially available CDPs that contain cross-linkers that impart negative and positive surface charges, respectively. amine-CDP was synthesized as previously described and contains cross-linkers that impart a positive surface charge at circumneutral pH values;<sup>39</sup> details on the amine-CDP synthesis procedure are provided in text in the Supporting Information and a characterization of the pore size distribution is provided in Figure S1. Purofine PFA694E (Purofine, Philadelphia, PA) is a commercially available AE resin functionalized with complex amino groups and marketed for PFAS removal from water.<sup>53</sup> Purofine PFC100E (Purofine, Philadelphia, PA) is a commercially available CE resin that contains aryl sulfonic acid groups and is marketed for potable water softening.<sup>54</sup> Further details on the adsorbents including particle size, surface area, and zeta potential are provided in Table S2 of the Supporting Information.

**Batch Experiments.** A fixed volume of the stock mixture solution (1 mg L<sup>−1</sup>) containing the eleven PFASs was added to sacrificial polypropylene centrifuge tubes containing 12 mL of nanopure water or groundwater to generate the desired initial PFAS concentration ( $[PFAS]_0 = 1 \mu\text{g L}^{-1}$  unless otherwise noted) and mixed on a tube revolver (Thermo Fisher Scientific) at 40 rpm at 23 °C overnight. Adsorbents were then added to the centrifuge tubes to the desired dose ( $[adsorbent]_0 = 10 \text{ mg L}^{-1}$  unless otherwise noted). Prior to adding CDPs to the centrifuge tube, each CDP was rehydrated to create a homogeneous, aqueous suspension. To rehydrate the CDPs, nanopure water was added to a 20 mL amber vial containing approximately 10 mg of the adsorbent to create a 1

$\text{g L}^{-1}$  aqueous suspension. The vial was capped, sonicated for 1 min, and stirred on a multiposition stirrer (VWR) for 1 h at 460 rpm at 23 °C.<sup>35,38</sup> The ion-exchange resins were massed and added directly to each centrifuge tube. At selected time points, 8 mL of the reactor volume was filtered through a 0.45  $\mu\text{m}$  cellulose acetate filter (Restek) into a 10 mL glass LCMS vial and spiked with a mixture of six isotope-labeled internal standards (ILISs); we note that limited PFAS losses were observed in recovery experiments with the 0.45  $\mu\text{m}$  cellulose acetate filters. For batch experiments targeting adsorption kinetics, samples were taken at 0.5, 9, and 48 h. For batch experiments targeting adsorbent affinity, samples were taken at 48 h under the standard initial conditions of  $[\text{PFAS}]_0 = 1 \mu\text{g L}^{-1}$  and  $[\text{adsorbent}]_0 = 10 \text{ mg L}^{-1}$  and also at  $[\text{PFAS}]_0 = 2 \mu\text{g L}^{-1}$  and  $[\text{adsorbent}]_0 = 10, 25, \text{ and } 50 \text{ mg L}^{-1}$  to explore the linear region of the adsorption isotherm. To evaluate the effect of pH on PFAS adsorption, samples were taken at 48 h and the nanopure water was modified with drops of 0.1 M HCl and 0.1 M NaOH to adjust the pH to 5.5, 7, and 8.5. To evaluate the effect of water matrix constituents on PFAS adsorption, samples were taken at 48 h and experiments were conducted in groundwater with pH likewise adjusted to 5.5, 7, and 8.5. All batch experiments were performed in triplicate alongside triplicate control experiments conducted under the same conditions but in the absence of the adsorbent.

**Analytical Method.** Samples were measured using large-volume injection by means of HPLC-MS/MS as previously described (QExactive, Thermo Fisher Scientific).<sup>38,39,43,55</sup> Briefly, the mobile phase consisted of (A) LCMS-grade water amended with 20 mM ammonium acetate and (B) LCMS-grade methanol. Samples were injected at 5 mL volumes onto a Hypersil Gold dC18 12  $\mu\text{m}$  2.1  $\times$  20 mm trap column (Thermo Fisher Scientific) and eluted onto an Atlantis dC18 5  $\mu\text{m}$  2.1  $\times$  150 mm analytical column (Waters). The mobile phase was delivered starting at 40% B at 300  $\mu\text{L min}^{-1}$ . The fraction of B in the mobile phase increased linearly for 24 min until 90% B at 30 min; 90% B was held for 7 min before returning to 40% B at 37 min. The HPLC-MS was operated with electrospray ionization in the positive and negative polarity mode. The neutral mass formula, the neutral mass, the dominant adduct, the extract mass, the retention time, and the selected ILISs for each target PFAS are provided in Table S3. An eleven-point, matrix-matched calibration curve with concentrations ranging from 0 to 2000  $\text{ng L}^{-1}$  was prepared for the quantification of PFASs in samples from the kinetics and affinity experiments for all adsorbents, and the experiments were designed to address effects of pH and matrix constituents for the CE resin. A ten-point, matrix-matched calibration curve with concentrations ranging from 0 to 1500  $\text{ng L}^{-1}$  was prepared for the quantification of PFASs in samples from the experiments designed to address effects of pH and matrix constituents for DEXSORB, DEXSORB+, amine-CDP, and the AE resin. Analytes were quantified from the calibration standards based on the PFAS target-to-ILIS peak area ratio responses by linear least-squares regression. Calibration curves were run at the beginning of the analytical run. Instrument blanks were run before and after the calibration curve and each batch of triplicate samples. Limits of quantification (LOQs) for each PFAS were determined as the lowest point on the calibration curve with at least five MS scans and a PFAS target-to-ILIS peak area ratio that could be distinguished from the blank.<sup>43</sup> Concentrations measured below the LOQ were conservatively redefined as the LOQ when calculating

adsorption density and removal. The coefficient of determination ( $R^2$ ) and LOQ for each PFAS in each experiment are provided in Table S4.

**Data Analysis.** PFAS removal was determined as described in eq 1

$$\% \text{ removal} = \frac{C_0 - C_t}{C_0} \times 100 \quad (1)$$

where  $C_0$  [ $\text{ng L}^{-1}$ ] is the average concentration of a given PFAS in the control samples and  $C_t$  [ $\text{ng L}^{-1}$ ] is the concentration of the PFAS in the sample at time  $t$ . Any incidental PFAS losses were assumed to occur to the same extent in control and experimental treatments and were therefore not explicitly considered in eq 1. Adsorption density was calculated as described in eq 2

$$q_t = \frac{C_0 - C_t}{C_{\text{ads}}} \quad (2)$$

where  $q_t$  [ $\mu\text{g g}^{-1}$ ] is the adsorption density at time  $t$ ,  $C_0$  [ $\text{ng L}^{-1}$ ] is the average concentration of a given PFAS in the control samples,  $C_t$  [ $\text{ng L}^{-1}$ ] is the concentration of the PFAS in the sample at time  $t$ , and  $C_{\text{ads}}$  [ $\text{mg L}^{-1}$ ] is the concentration of the adsorbent used in the experiment. The distribution coefficient ( $K_D$ ) was calculated as

$$K_D = 1000 \times \frac{q_t}{C_t} \quad (3)$$

where  $K_D$  is in units of  $\text{L g}^{-1}$  and was calculated at  $t = 48 \text{ h}$ . The R Statistical Software v3.5.2 was used to compute analysis of variance (ANOVA) and Tukey's honest significance difference (Tukey-HSD) to assess differences among experimental groups ( $p < 0.01$ ).

## RESULTS AND DISCUSSION

**Adsorption Kinetics.** We first characterized the adsorption kinetics of the 11 target PFASs on each of the five adsorbents. Data describing adsorption kinetics provide insight on how long it takes for a particular adsorption process to reach equilibrium. Adsorption kinetics experiments also enable evaluation of desorption, which is an important consideration when evaluating PFAS adsorption on any adsorbent; it is often reported that short-chain PFASs will desorb after an initial period of rapid adsorption.<sup>22,30</sup> The results of our batch kinetics experiments are presented in Figure 1 as a time series detailing the average and standard deviation (%) of the removal for each of the 11 PFASs by each adsorbent at 0.5, 9, and 48 h. Although the adsorption kinetics of the four anionic PFASs have been previously explored for a variety of adsorbents,<sup>33,39,43,56</sup> this is the first known study evaluating the adsorption kinetics of the three zwitterionic PFASs and the four nonionic PFASs using CDPs and ion-exchange resins.

DEXSORB exhibits rapid adsorption of the three zwitterionic PFASs (64% average removal for AmPr-FHxSA, 56% for TAmPr-FHxSA, and 47% for 6:2 FTSA-PrB in 0.5 h) and adsorption equilibrium is attained within 9 h; the adsorption of the three zwitterionic PFASs is stable at 9 h and 48 h ( $p < 0.01$ ) with a removal of approximately 75%. The CE resin likewise exhibits rapid adsorption of AmPr-FHxSA and TAmPr-FHxSA (50% average removal for AmPr-FHxSA and 48% for TAmPr-FHxSA in 0.5 h) followed by continued slow removal to achieve approximately 71% removal at 48 h. However, relatively slow removal was observed for 6:2 FTSA-

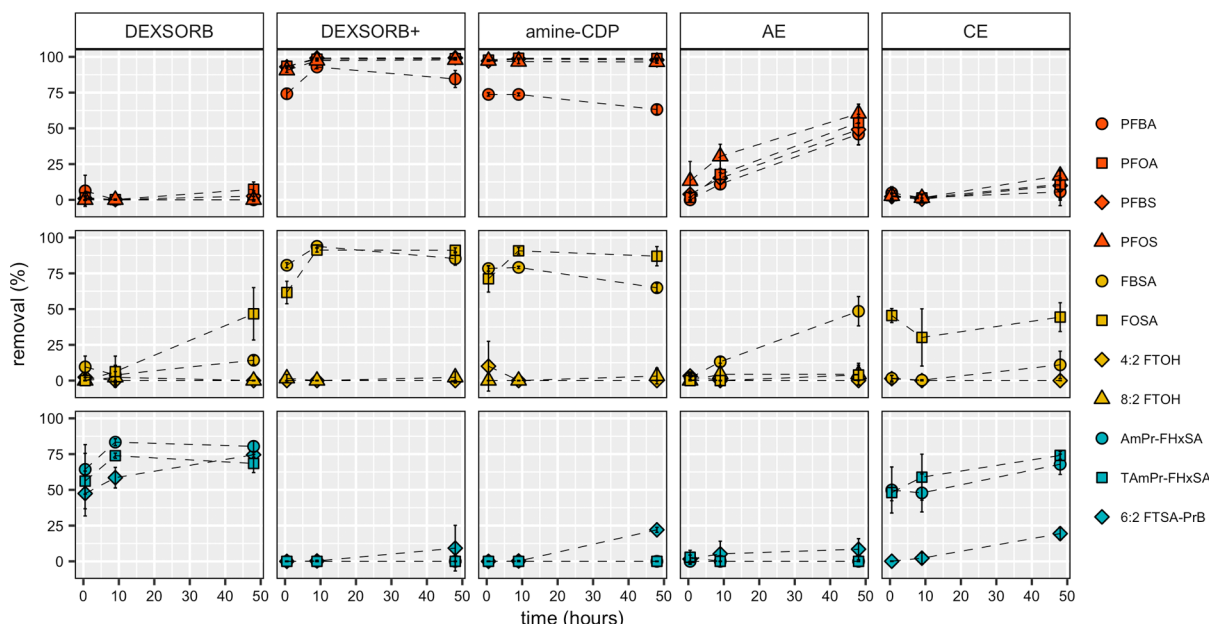


**Figure 1.** Average and standard deviation (%) of triplicate measurements of removal of each PFAS on each adsorbent after 0.5, 9, and 48 h of contact time. The kinetics experiments were conducted at  $[PFAS]_0 = 1 \mu\text{g L}^{-1}$  and  $[adsorbent]_0 = 10 \text{ mg L}^{-1}$ .

PrB, with no removal observed at 0.5 h and only 19% average removal attained at 48 h. None of the other adsorbents exhibit rapid removal of any zwitterionic PFASs, with amine-CDP exhibiting only slow removal of 6:2 FTSA-PrB and attaining only 22% average removal after 48 h. The high and rapid removal of all three zwitterionic PFASs by DEXSORB suggests that DEXSORB is better suited to remove zwitterionic PFASs than the other adsorbents, although the CE resin also shows promise for removing some zwitterionic PFASs from water. DEXSORB also exhibits relatively slow removal of FBSA and FOSA, reaching 14% and 47% average removal by 48 h, respectively; these observations demonstrate the potential of DEXSORB to remove nonionic PFASs from water. The CE resin also exhibits some removal of FOSA but no removal of FBSA. The remaining anionic PFASs and nonionic PFASs are not removed to a significant extent by DEXSORB or the CE resin.

DEXSORB+ and amine-CDP exhibit rapid adsorption of the four anionic PFASs and the two nonionic perfluorosulfonamides (>62% average removal in 0.5 h). The adsorption of all six PFASs increases significantly at 9 h of contact time with DEXSORB+, reflecting slower adsorption kinetics for these PFASs. Equilibrium adsorption is achieved for all six PFASs on DEXSORB+ at 9 h with no significant desorption observed. In contrast, all six PFASs achieve complete adsorption uptake on amine-CDP at 0.5 h. However, some slight but significant desorption was observed for PFBA (~10%) and FBSA (~14%) after 48 h of contact time; desorption of short-chain anionic PFASs has been previously reported for activated carbon and has been attributed to competition with adsorbates with higher affinity.<sup>22,57</sup> In this case, competition with long-chain anionic PFASs or with 6:2 FTSA-PrB may have contributed to the noted desorption. Together, these data suggest that DEXSORB+ and amine-CDP are effective at rapidly removing anionic PFASs and two nonionic perfluorosulfonamides, although DEXSORB+ exhibits slower adsorption kinetics and amine-CDP exhibits some desorption potential.

In contrast to the three CDPs and the CE resin, the AE resin did not exhibit rapid adsorption of any of the PFASs. Instead, slowly increasing adsorption was observed for the four anionic PFASs and FBSA, reaching a maximum of 60% removal of PFOS and a minimum of 46% removal for PFBA at 48 h. We note that the relatively slow adsorption kinetics observed for the AE resins could be the result of the study design that relied on a fixed concentration of each adsorbent in its as-received morphology. The relatively large particle size of the AE resins (Table S2) likely played a role in the results of the kinetics experiments and improved adsorption kinetics are expected for higher doses of AE resins<sup>58</sup> or with modified (i.e., ground) AE resin particles.<sup>59</sup> Nevertheless, it is interesting to note steady adsorption of the four anionic PFASs and FBSA (but not FOSA) without any evidence of desorption; the data from the perfluorosulfonamides suggest that FBSA exhibits some anionic properties at circumneutral pH, whereas FOSA exhibits more nonionic adsorbate behavior.

None of the adsorbents removed the nonionic fluorotelomer alcohols to a significant extent. We note that these two PFASs were not reliably measured and had relatively high LOQs (Table S4). This may be due to the formation of poorly ionized acetate adducts in the mass spectrometer or other analytical challenges.<sup>60</sup> Regardless, it is worth noting that these nonionic PFASs with four- and eight-carbon perfluorinated chains are not well-removed by CDPs with either positive or negative surface charges or by ion-exchange resins. Other nonionic molecules have exhibited varying extents of affinity for CDPs but that variability has been positively associated with molecular size.<sup>35,40</sup> The noted adsorption of PFOA, PFOS, and FOSA among the CDPs suggests that 8:2 FTOH should be of sufficient size to interact with the interior cavity of the cyclodextrin monomer. We therefore suspect that the fluorotelomer alcohols may aggregate or accumulate at air–water interfaces (as has been demonstrated for other types of PFASs)<sup>61</sup> and may not be uniformly dissolved in the aquatic matrix which may limit their transport to the binding sites in the interior cavity of the cyclodextrin monomer.

**Adsorbent Affinity for Different PFASs.** We next characterized the affinity of each adsorbent for each of the 11 target PFASs. Although the affinity of adsorbents for any adsorbate is typically characterized by adsorption isotherms,<sup>62,63</sup> PFASs are present at low concentrations in groundwater so complete isotherms do not provide relevant data for this study.<sup>64</sup> Here, we use distribution coefficients ( $K_D$ ) calculated from data in the linear region of the adsorption isotherm to provide a better description of adsorption affinity at low concentrations.<sup>40,65</sup> We used data from our adsorption affinity experiments to calculate  $K_D$  values for each PFAS on each adsorbent. We used the experimental conditions of  $[PFAS]_0 = 2 \mu\text{g L}^{-1}$  and  $[\text{adsorbent}]_0 = 25 \text{ mg L}^{-1}$  to first define the  $K_D$  value and then incorporated data from other experimental scenarios for which the calculated  $K_D$  value was not statistically different from the defined  $K_D$  value. This conservative approach was implemented as a quality control measure to ensure that we were estimating constant  $K_D$  values that represent the linear range of the nonlinear isotherm.<sup>40,66</sup> In Figure 2, we plot the average  $\log K_D$  values and the relative error for each PFAS on each adsorbent. The  $\log K_D$  values used to generate Figure 2 are provided in Table S5.

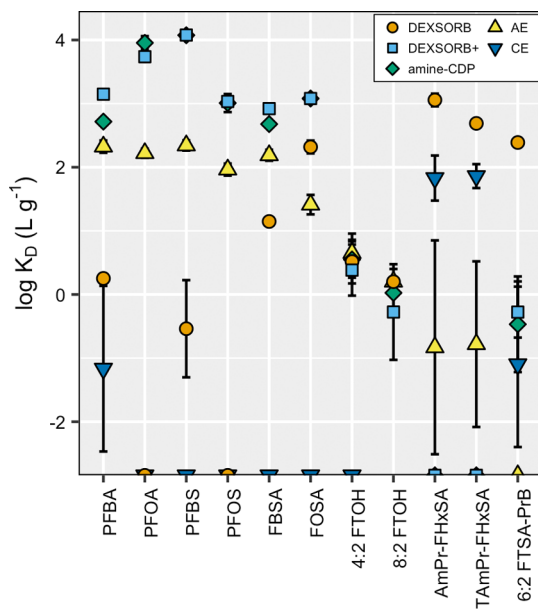


**Figure 2.** Plots of the average and relative error of the log-transformed distribution coefficients ( $\log K_D$ ) for 11 PFASs and five adsorbents. PFASs that are plotted in the lowest part of the panel have  $K_D$  values of  $0 \text{ g L}^{-1}$  (i.e., no affinity for the adsorbent). The PFAS-adsorbent concentrations that were tested were  $[PFAS]_0 = 1 \mu\text{g L}^{-1}$  and  $[\text{adsorbent}]_0 = 10 \text{ mg L}^{-1}$ ;  $[PFAS]_0 = 2 \mu\text{g L}^{-1}$  and  $[\text{adsorbent}]_0 = 10 \text{ mg L}^{-1}$ ;  $[PFAS]_0 = 2 \mu\text{g L}^{-1}$  and  $[\text{adsorbent}]_0 = 25 \text{ mg L}^{-1}$ ; and  $[PFAS]_0 = 2 \mu\text{g L}^{-1}$  and  $[\text{adsorbent}]_0 = 50 \text{ mg L}^{-1}$ . 8:2 FTOH was undetected in the control samples for the CE experiments and is not shown in the figure. When no error bars are visible, the error was smaller than the size of the data point.

DEXSORB exhibits moderate (average  $\log K_D > 2$  for TAmPr-FHxSA and 6:2 FTSA-PrB) to high (average  $\log K_D > 3$ ) affinity for the three zwitterionic PFASs. This is notable because none of the other adsorbents exhibit such affinity for the three zwitterionic PFASs; the CE resins have average  $\log K_D$  values of 1.8 and 1.9 for AmPr-FHxSA and TAmPr-FHxSA, respectively, but an average  $\log K_D$  value of  $-1.1$  for 6:2 FTSA-

PrB. This suggests that the cationic functional groups on the zwitterionic PFASs likely play an important role in determining their affinity for CDP adsorbents. Zwitterionic PFASs containing betaine or quaternary ammonium functional groups have been found to bind strongly to negatively charged soil particles<sup>67–70</sup> providing further evidence for the role that cationic functional groups play in the fate of zwitterionic PFASs. DEXSORB exhibits poor affinity for all four anionic PFASs (average  $\log K_D < 0.5$ ). This is expected, as we previously reported that a similar CDP with a negative surface charge exhibits poor removal of PFBA and PFOA.<sup>35,41</sup> Interestingly, DEXSORB has average  $\log K_D$  values of 1.1 and 2.3 for the nonionic perfluorosulfonamides FBSA and FOSA, respectively, but poor affinity for the fluorotelomer alcohols (4:2 FTOH and 8:2 FTOH). The variable affinity of DEXSORB for nonionic PFASs agrees with our previous observations of variable removal of nonionic micropollutants by CDPs;<sup>35,39–41</sup> furthermore, the moderate affinity for the perfluorosulfonamides suggests either that some significant fraction of these PFASs is indeed nonionic at circumneutral pH or that the negative charge of the deprotonated sulfonamide group is insufficient to limit their affinity for DEXSORB.

DEXSORB+ and amine-CDP exhibit high affinity (average  $\log K_D > 3$ ) for the four anionic PFASs, with the exception being an average  $\log K_D$  value of 2.7 for PFBA on amine-CDP. This high affinity is expected, as we previously reported that DEXSORB+ and amine-CDP exhibit generally good removal of anionic PFASs.<sup>39,43</sup> DEXSORB+ and amine-CDP also exhibit moderate affinity for FBSA and high affinity for FOSA, with a notable improvement of affinity for FBSA relative to DEXSORB. The improved affinity of the sulfonamides for the CDPs with a positive surface charge suggests that electrostatic interactions are important to some degree and that some fraction of the sulfonamides may be anionic as suggested by their estimated  $pK_a$  values (Table S1). Finally, DEXSORB+ and amine-CDP exhibit poor affinity (average  $\log K_D < 0.5$ ) for the zwitterionic PFASs and the fluorotelomer alcohols.

The AE resin exhibits moderate affinity (average  $\log K_D > 2$ ) for the four anionic PFASs and FBSA. FBSA exhibits identical affinity for the AE resin as PFBA, providing further evidence that FBSA is at least partially anionic at circumneutral pH and relies on electrostatic interactions to be removed by the adsorbents. Interestingly, FOSA has an average  $\log K_D$  value of 1.4 on the AE resin providing additional evidence that FOSA is more nonionic at circumneutral pH and relies more on hydrophobic interactions with the CDP adsorbents. The AE resin exhibits poor affinity for the fluorotelomer alcohols and zwitterionic PFASs. We note that our experimental design limits our ability to compare the absolute values of affinity for the AE resin with the values reported for the CDPs. The CDPs have a greater external surface area and may result in more rapid equilibration than the AE resins (Table S2); previous studies evaluating AE resins ground the resins into smaller particles,<sup>59</sup> used greater concentrations of the resins,<sup>29,31</sup> or relied on contact times up to 10 days to evaluate their performance.<sup>29</sup>

**Effects of pH on PFAS Adsorption.** We next explored the effects of pH and water matrix constituents on the adsorption of PFASs on each of the five adsorbents. We performed batch equilibrium experiments across a gradient of environmentally relevant pH values (5.5, 7, and 8.5) to measure the removal of each PFAS at 48 h in nanopure and groundwater. We exclude

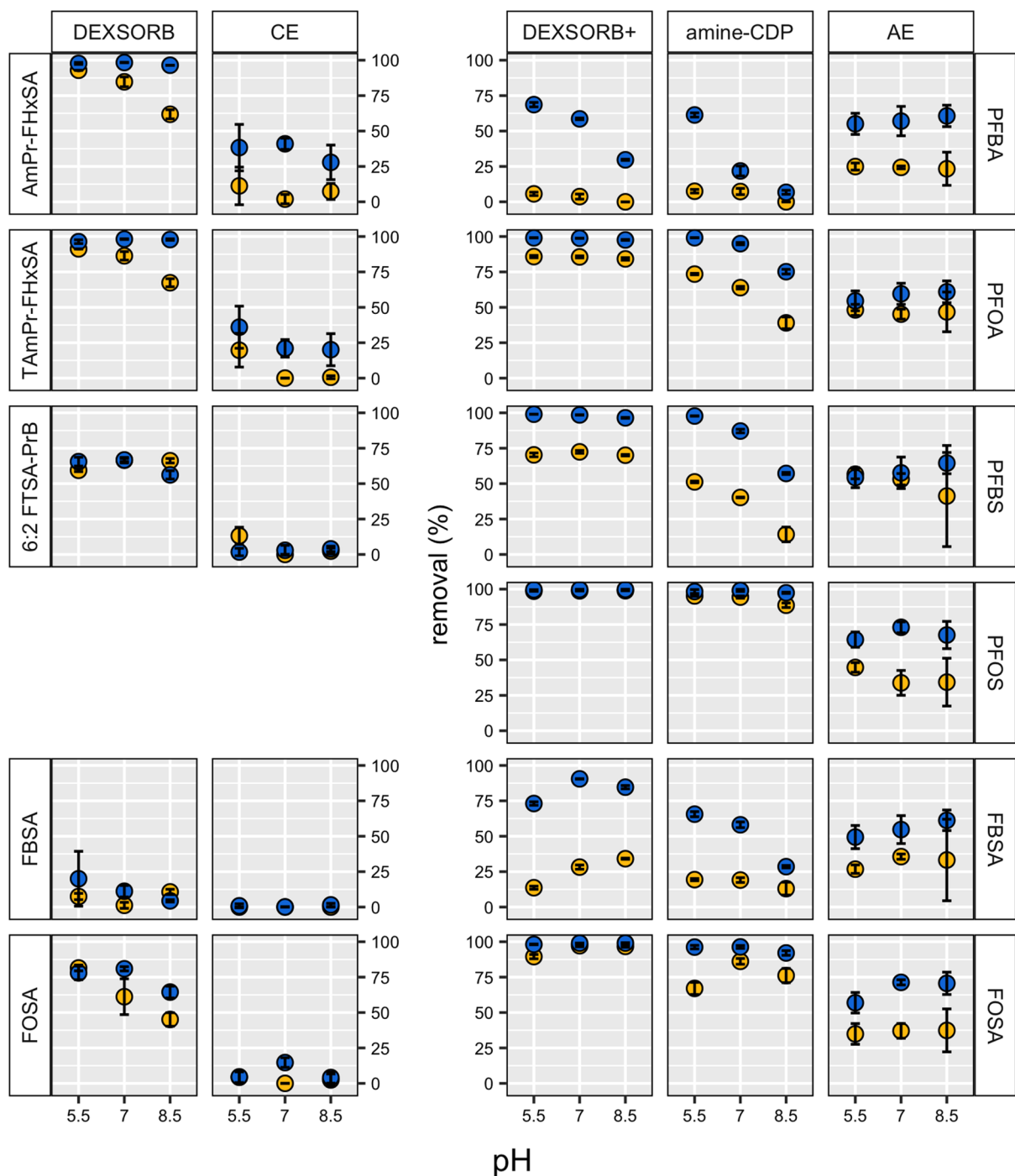


**Figure 3.** Average removal of PFASs by adsorbents that had nonnegligible removal. Effects of pH and matrix constituents were evaluated at pH 5.5, 7, and 8.5. Blue = nanopure water, yellow = groundwater. Samples were collected after a contact time of 48 h, with  $[PFAS]_0 = 1 \mu\text{g L}^{-1}$  and  $[\text{adsorbent}]_0 = 10 \text{ mg L}^{-1}$ .

4:2 FTOH and 8:2 FTOH from our data analysis because the analytical data did not meet our quality control criteria (Table S4). The data presented in Figure 3 show the removal of each of the remaining nine PFASs at each pH value in a nanopure matrix (blue) and in a groundwater matrix (yellow); data for PFASs that were not removed on certain adsorbents are not shown in Figure 3.

pH influences the surface chemistry and surface charge of adsorbents and also influences the speciation of adsorbates. According to estimated  $pK_a$  values for each of the nine PFASs included in this part of our study (Table S1), the four anionic

PFASs should remain anionic over the pH range studied, but the other PFASs may experience some changes in speciation.<sup>49,50,52</sup> The predicted  $pK_a$  values for the perfluorosulfonamides range between 3.3 and 6.6.<sup>49,52</sup> Our data from the affinity and kinetics experiments show that the perfluorosulfonamides exhibit behavior that resembles both anionic PFASs (particularly for FBSA) and nonionic micropollutants (particularly, for FOSA). Therefore, the  $pK_a$  of FOSA is likely closer to 6.6 and the  $pK_a$  for FBSA is likely somewhat lower. Nevertheless, we expect that both FBSA and FOSA will be more nonionic at lower pH values and more anionic at higher

pH values. The three zwitterionic PFASs are all expected to be zwitterionic at circumneutral pH. However, all three could become cations at lower pH values; AmPr-FHxSA is an anion at higher pH values, and 6:2 FTSA-PrB has a second acidic group that can deprotonate at higher pH values (see Table S6 for structures and speciation estimates for the zwitterionic PFASs). As for the adsorbents, DEXSORB incorporates weakly acidic functional groups in the cross-linker and can therefore become deprotonated (i.e., more negative) with increasing pH;<sup>71</sup> our measurements of zeta potential demonstrate that the surface charge of DEXSORB is significantly more negative at pH 8.5 (Table S2). amine-CDP incorporates weakly basic functional groups in the cross-linker and can likewise become deprotonated (i.e., less positive) with increasing pH.<sup>39</sup> However, no significant change in zeta potential was noted for amine-CDP at the different pH values (Table S2) suggesting that the  $pK_a$  value of the weakly basic amine groups is greater than 8.5. The AE resin contains complex amino groups that can likewise deprotonate with increasing pH and adsorption on the AE resin may consequently be influenced by pH changes.<sup>72</sup> DEXSORB+ and the CE resin do not contain weakly acidic or basic functional groups, so the surface charge is not influenced by changes in pH (Table S2).

The top-left region of Figure 3 shows the average removal of the zwitterionic PFASs as a function of pH on DEXSORB and the CE resin in nanopure water (blue); the other three adsorbents are not included in the analysis because removal of zwitterionic PFASs on DEXSORB+, amine-CDP, and the AE resin was negligible. We expect lower pH values to change the speciation of the zwitterionic PFAS to be more cationic, whereas higher pH values will change the speciation of AmPr-FHxSA and 6:2 FTSA-PrB making them more anionic while strengthening the negative surface charge of DEXSORB. Our results suggest that these changes in speciation resulting from changes in pH have no significant effect on the adsorption of zwitterionic PFASs on DEXSORB and the CE resin in nanopure water, as no significant changes in removal of the zwitterionic PFASs on DEXSORB and the CE resin were observed across the tested pH range ( $p < 0.01$ ).

The top-right region of Figure 3 shows the average removal of the anionic PFASs as a function of pH on DEXSORB+, amine-CDP, and the AE resin in nanopure water (blue); DEXSORB and the CE resin are not included in the analysis because removal of anionic PFASs on DEXSORB and the CE resin was negligible. The data here demonstrate that adsorption of anionic PFASs on the AE resin is not significantly dependent on the pH ( $p < 0.01$ ), although a previous study reported adsorption inhibition of anionic PFASs for AE resins (functionalized with tertiary amine groups) because of the decreased adsorption sites at higher pH.<sup>72</sup> Conversely, the adsorption of some anionic PFASs on DEXSORB+ and amine-CDP is pH-dependent; this pH dependency is determined by the chain length and head group of the PFAS. For DEXSORB+, only the adsorption of PFBA is significantly influenced by pH with 70% removal observed at pH 5.5 and 30% removal observed at pH 8.5. A more dramatic influence of pH is noted for amine-CDP, with the adsorption of PFBA, PFOA, and PFBS all significantly inhibited with increasing pH. Although no statistically significant change in zeta potential was observed for amine-CDP across the gradient of pH values investigated, the adsorption inhibition on amine-CDP may still be linked to some deprotonation of surface functional groups at increasing

pH values. The adsorption inhibition on DEXSORB+ is not attributable to deprotonation of surface functional groups and is therefore attributed to competition of cationic surface sites with an increased abundance of hydroxide anions at higher pH values.

The bottom region of Figure 3 shows the average removal of the nonionic perfluorosulfonamides as a function of pH on all five adsorbents in nanopure water (blue). We expect that these perfluorosulfonamides will be mostly neutral at a pH of 5.5 and at least partly anionic at pH 8.5. The data here demonstrate again that the adsorption of perfluorosulfonamides on ion-exchange resins is not pH-dependent ( $p < 0.01$ ). However, some interesting trends emerge among the CDPs. DEXSORB does not remove FBSA to a significant extent at any pH, but DEXSORB removes FOSA better at pH 5.5 and 7, when FOSA is expected to be more nonionic. At pH 8.5, FOSA is expected to be more anionic and the surface charge of DEXSORB is more negative. Therefore, the adsorption inhibition observed here is likely due to the emergence of repulsive electrostatic interactions. The adsorption of FOSA on DEXSORB+ and amine-CDP is not significantly influenced by pH, suggesting that the increasingly anionic FOSA (at increasing pH) maintains a high affinity for the permanently positively charged DEXSORB+ and amine-CDP. On the other hand, the adsorption of FBSA on amine-CDP is significantly inhibited at increasing pH values, suggesting that some deprotonation of amine-CDP may contribute to the significant adsorption inhibition of FBSA.

#### Effects of Matrix Constituents on PFAS Adsorption.

We also evaluated the performance of each adsorbent in a real groundwater matrix. The groundwater selected for these experiments contained no background levels of any of the PFASs included in the study and had an in situ pH of 8.4. We adjusted the pH of the groundwater in the same way we adjusted the pH of the nanopure, and therefore, the results presented in Figure 3 (groundwater = yellow) describe differences that can be attributed to the presence of inorganic anions, inorganic cations, and NOM. Data on the abundance of these constituents in the groundwater are provided in Table S7.

The data presented in Figure 3 show that the presence of matrix constituents significantly inhibited the adsorption of most of the PFASs on each of the adsorbents. The adsorption inhibition noted for the AE resin was most likely resulting from the presence of inorganic anions<sup>31,32</sup> and NOM<sup>21,30</sup> that compete with PFASs for adsorption sites on the resin; sulfate (18.7 mg L<sup>-1</sup>) and chloride (8.9 mg L<sup>-1</sup>) were the most abundant anions measured in the groundwater, and the NOM concentration was 1.1 mg L<sup>-1</sup>. On the other hand, the adsorption inhibition noted for the CE resin, particularly, for AmPr-FHxSA and TAmPr-FHxSA, is attributed to the presence of inorganic cations including calcium (26.8 mg L<sup>-1</sup>) and sodium (23.2 mg L<sup>-1</sup>). DEXSORB was the least inhibited adsorbent in the groundwater matrix and the adsorption of 6:2 FTSA-PrB was not inhibited at any pH value. Interestingly, the adsorption of AmPr-FHxSA and TAmPr-FHxSA was inhibited at higher pH values in groundwater but not in nanopure water, suggesting that speciation of matrix constituents was responsible for the adsorption inhibition; it is possible that anionic NOM could interact with the positive charge on the zwitterionic PFAS to contribute to adsorption inhibition. Finally, adsorption of most of the anionic and neutral PFAS on DEXSORB+ and amine-

CDP was significantly inhibited in the groundwater; only the adsorption of PFOS and FOSA on DEXSORB+ was not significantly inhibited in groundwater. We expect that interferences caused by the presence of inorganic ions and low-molecular-weight NOM may be driving adsorption inhibition in groundwater.<sup>42,43</sup>

**Environmental Implications.** This study offers the first systematic exploration on the performance of emerging adsorbent technologies, including CDPs and ion-exchange resins, for the removal of different classes of PFASs from water. We found that DEXSORB (a CDP with a negative surface charge) exhibits the best performance for removing zwitterionic PFASs from groundwater. Our findings show that zwitterionic PFASs behave more similarly to cations than anions, which can have important implications in evaluating other remediation technologies, including adsorption with CE resins. We also demonstrated that nonionic PFASs (perfluorosulfonamides and fluorotelomer alcohols) are removed to varying degrees by CDPs but are generally not removed well by ion-exchange resins. Although the latter observation was expected, it was not expected that neutral PFASs of the appropriate size would not be removed by CDPs. These data suggest that electrostatic interactions play an important role in determining the affinity of CDPs for PFASs. Although all adsorbents exhibited some level of inhibition in real groundwater, a combination of adsorbents could be used to remove complex mixtures of PFASs from contaminated groundwater. Finally, we note that previous studies with CDPs have also demonstrated facile regeneration and reuse potential in proof-of-concept experiments.<sup>34,36</sup> These observations, coupled with the findings of the present study, support the continued investigation of CDPs as alternative adsorbents for remediation of PFAS-contaminated groundwater.

## ASSOCIATED CONTENT

### Supporting Information

The Supporting Information is available free of charge at <https://pubs.acs.org/doi/10.1021/acs.est.0c04028>.

Chemicals and reagents, adsorbents, analytical method, adsorbent affinity for different PFASs, effects of pH on PFAS adsorption, and effects of matrix constituents on PFAS adsorption ([PDF](#))

## AUTHOR INFORMATION

### Corresponding Authors

**William R. Dichtel** — *Department of Chemistry, Northwestern University, Evanston, Illinois 60208, United States*  
✉ [orcid.org/0000-0002-3635-6119](https://orcid.org/0000-0002-3635-6119); Phone: +1 847 467 6031; Email: [wdichtel@northwestern.edu](mailto:wdichtel@northwestern.edu)

**Damian E. Helbling** — *School of Civil and Environmental Engineering, Cornell University, Ithaca, New York 14853, United States*; ✉ [orcid.org/0000-0003-2588-145X](https://orcid.org/0000-0003-2588-145X); Phone: +1 607 255 5146; Email: [damian.helbling@cornell.edu](mailto:damian.helbling@cornell.edu)

### Authors

**Casey Ching** — *School of Civil and Environmental Engineering, Cornell University, Ithaca, New York 14853, United States*

**Max J. Klemes** — *Department of Chemistry, Northwestern University, Evanston, Illinois 60208, United States*; ✉ [orcid.org/0000-0002-4481-890X](https://orcid.org/0000-0002-4481-890X)

**Brittany Trang** — *Department of Chemistry, Northwestern University, Evanston, Illinois 60208, United States*

Complete contact information is available at: <https://pubs.acs.org/10.1021/acs.est.0c04028>

### Notes

The authors declare the following competing financial interest(s): W.R.D and D.E.H own equity and/or stock options in CycloPure Inc., which is commercializing cyclo-dextrin-based polymers related to those reported in this work.

## ACKNOWLEDGMENTS

The study was supported by the Center for Sustainable Polymers (CSP), a National Science Foundation (NSF)-supported Center for Chemical Innovation (CHE-1413862), and by the Strategic Environmental Research and Development Program (ER18-1026).

## REFERENCES

- (1) Buck, R. C.; Franklin, J.; Berger, U.; Conder, J. M.; Cousins, I. T.; de Voogt, P.; Jensen, A. A.; Kannan, K.; Mabury, S. A.; van Leeuwen, S. P. Perfluoroalkyl and Polyfluoroalkyl Substances in the Environment: Terminology, Classification, and Origins. *Integr. Environ. Assess. Manage.* **2011**, *7*, 513–541.
- (2) Wang, Z.; Dewitt, J. C.; Higgins, C. P.; Cousins, I. T. A Never-Ending Story of Per- and Polyfluoroalkyl Substances (PFASs)? *Environ. Sci. Technol.* **2017**, *51*, 2508–2518.
- (3) OECD. *Synthesis Paper on Per- and Polyfluorinated Chemicals (PFCs), Environment, Health and Safety*, Environment Directorate, OECD; OECD/UNEP Global PFC Group, 2013.
- (4) Dewitt, J. C. *Human Health Risk Assessment of Perfluoroalkyl Acids*; Humana Press, 2015.
- (5) Hu, X. C.; Andrews, D. Q.; Lindstrom, A. B.; Bruton, T. A.; Schaefer, L. A.; Grandjean, P.; Lohmann, R.; Carignan, C. C.; Blum, A.; Balan, S. A.; Higgins, C. P.; Sunderland, E. M. Detection of Poly- and Perfluoroalkyl Substances (PFASs) in U.S. Drinking Water Linked to Industrial Sites, Military Fire Training Areas, and Wastewater Treatment Plants. *Environ. Sci. Technol. Lett.* **2016**, *3*, 344–350.
- (6) Backe, W. J.; Day, T. C.; Field, J. A. Zwitterionic, Cationic, and Anionic Fluorinated Chemicals in Aqueous Film Forming Foam Formulations and Groundwater from U.S. Military Bases by Nonaqueous Large-Volume Injection HPLC-MS/MS. *Environ. Sci. Technol.* **2013**, *47*, 5226–5234.
- (7) Barzen-Hanson, K. A.; Roberts, S. C.; Choyke, S.; Oetjen, K.; McAlees, A.; Riddell, N.; McCrindle, R.; Ferguson, P. L.; Higgins, C. P.; Field, J. A. Discovery of 40 Classes of Per- and Polyfluoroalkyl Substances in Historical Aqueous Film-Forming Foams (AFFFs) and AFFF-Impacted Groundwater. *Environ. Sci. Technol.* **2017**, *51*, 2047–2057.
- (8) Mejia-Avendaño, S.; Munoz, G.; Vo Duy, S.; Desrosiers, M.; Benoit, P.; Sauvé, S.; Liu, J. Novel Fluoroalkylated Surfactants in Soils Following Firefighting Foam Deployment during the Lac-Mégantic Railway Accident. *Environ. Sci. Technol.* **2017**, *51*, 8313–8323.
- (9) Munoz, G.; Duy, S. V.; Labadie, P.; Botta, F.; Budzinski, H.; Lestremau, F.; Liu, J.; Sauvé, S. Analysis of Zwitterionic, Cationic, and Anionic Poly- and Perfluoroalkyl Surfactants in Sediments by Liquid Chromatography Polarity-Switching Electrospray Ionization Coupled to High Resolution Mass Spectrometry. *Talanta* **2016**, *152*, 447–456.
- (10) Moe, M. K.; Huber, S.; Svenson, J.; Hagenaars, A.; Pabon, M.; Trümper, M.; Berger, U.; Knapen, D.; Herzke, D. The Structure of the Fire Fighting Foam Surfactant Forafac1157 and Its Biological and Photolytic Transformation Products. *Chemosphere* **2012**, *89*, 869–875.
- (11) D'Agostino, L. A.; Mabury, S. A. Identification of Novel Fluorinated Surfactants in Aqueous Film Forming Foams and

Commercial Surfactant Concentrates. *Environ. Sci. Technol.* **2014**, *48*, 121–129.

(12) Dauchy, X.; Boiteux, V.; Colin, A.; Hémard, J.; Bach, C.; Rosin, C.; Munoz, J.-F. Deep Seepage of Per- and Polyfluoroalkyl Substances through the Soil of a Firefighter Training Site and Subsequent Groundwater Contamination. *Chemosphere* **2019**, *214*, 729–737.

(13) Li, Y.; Yu, N.; Du, L.; Shi, W.; Yu, H.; Song, M.; Wei, S. Transplacental Transfer of Per- and Polyfluoroalkyl Substances Identified in Paired Maternal and Cord Sera Using Suspect and Nontarget Screening. *Environ. Sci. Technol.* **2020**, *54*, 3407–3416.

(14) Xiao, F.; Hanson, R. A.; Golovko, S. A.; Golovko, M. Y.; Arnold, W. A. PFOA and PFOS Are Generated from Zwitterionic and Cationic Precursor Compounds During Water Disinfection with Chlorine or Ozone. *Environ. Sci. Technol. Lett.* **2018**, *5*, 382–388.

(15) Mejia-Avendaño, S.; Vo Duy, S.; Sauvé, S.; Liu, J. Generation of Perfluoroalkyl Acids from Aerobic Biotransformation of Quaternary Ammonium Polyfluoroalkyl Surfactants. *Environ. Sci. Technol.* **2016**, *50*, 9923–9932.

(16) McGuire, M. E.; Schaefer, C.; Richards, T.; Backe, W. J.; Field, J. A.; Houtz, E.; Sedlak, D. L.; Guelfo, J. L.; Wunsch, A.; Higgins, C. P. Evidence of Remediation-Induced Alteration of Subsurface Poly- and Perfluoroalkyl Substance Distribution at a Former Firefighter Training Area. *Environ. Sci. Technol.* **2014**, *48*, 6644–6652.

(17) Zhang, D. Q.; Zhang, W. L.; Liang, Y. N. Adsorption of Perfluoroalkyl and Polyfluoroalkyl Substances (PFASs) from Aqueous Solution - A Review. *Sci. Total Environ.* **2019**, *694*, 133606.

(18) Crone, B. C.; Speth, T. F.; Wahman, D. G.; Smith, S. J.; Abulikemu, G.; Kleiner, E. J.; Pressman, J. G. Occurrence of Per- and Polyfluoroalkyl Substances (PFAS) in Source Water and Their Treatment in Drinking Water. *Crit. Rev. Environ. Sci. Technol.* **2019**, *49*, 2359–2396.

(19) Du, Z.; Deng, S.; Bei, Y.; Huang, Q.; Wang, B.; Huang, J.; Yu, G. Adsorption Behavior and Mechanism of Perfluorinated Compounds on Various Adsorbents—A Review. *J. Hazard. Mater.* **2014**, *274*, 443–454.

(20) Merino, N.; Qu, Y.; Deeb, R. A.; Hawley, E. L.; Hoffmann, M. R.; Mahendra, S. Degradation and Removal Methods for Perfluoroalkyl and Polyfluoroalkyl Substances in Water. *Environ. Eng. Sci.* **2016**, *33*, 615–649.

(21) Kothawala, D. N.; Köhler, S. J.; Östlund, A.; Wiberg, K.; Ahrens, L. Influence of Dissolved Organic Matter Concentration and Composition on the Removal Efficiency of Perfluoroalkyl Substances (PFASs) during Drinking Water Treatment. *Water Res.* **2017**, *121*, 320–328.

(22) McCleaf, P.; Englund, S.; Östlund, A.; Lindegren, K.; Wiberg, K.; Ahrens, L. Removal Efficiency of Multiple Poly- and Perfluoroalkyl Substances (PFASs) in Drinking Water Using Granular Activated Carbon (GAC) and Anion Exchange (AE) Column Tests. *Water Res.* **2017**, *120*, 77–87.

(23) Rodowa, A. E.; Knappe, D. R. U.; Chiang, S.-Y. D.; Pohlmann, D.; Varley, C.; Bodour, A.; Field, J. A. Pilot Scale Removal of Per- and Polyfluoroalkyl Substances and Precursors from AFFF-Impacted Groundwater by Granular Activated Carbon. *Environ. Sci.: Water Res. Technol.* **2020**, *6*, 1083–1094.

(24) Gagliano, E.; Sgroi, M.; Falciglia, P. P.; Vagliasindi, F. G. A.; Roccaro, P. Removal of Poly- and Perfluoroalkyl Substances (PFAS) from Water by Adsorption: Role of PFAS Chain Length, Effect of Organic Matter and Challenges in Adsorbent Regeneration. *Water Res.* **2020**, *171*, 115381.

(25) Kennedy, A. M.; Reinert, A. M.; Knappe, D. R. U.; Ferrer, I.; Summers, R. S. Full- and Pilot-Scale GAC Adsorption of Organic Micropollutants. *Water Res.* **2015**, *68*, 238–248.

(26) Rossner, A.; Snyder, S. A.; Knappe, D. R. U. Removal of Emerging Contaminants of Concern by Alternative Adsorbents. *Water Res.* **2009**, *43*, 3787–3796.

(27) Quinlivan, P. A.; Li, L.; Knappe, D. R. U. Effects of Activated Carbon Characteristics on the Simultaneous Adsorption of Aqueous Organic Micropollutants and Natural Organic Matter. *Water Res.* **2005**, *39*, 1663–1673.

(28) Haddad, M.; Oie, C.; Vo Duy, S.; Sauvé, S.; Barbeau, B. Adsorption of Micropollutants Present in Surface Waters onto Polymeric Resins: Impact of Resin Type and Water Matrix on Performance. *Sci. Total Environ.* **2019**, *660*, 1449–1458.

(29) Maimaiti, A.; Deng, S.; Meng, P.; Wang, W.; Wang, B.; Huang, J.; Wang, Y.; Yu, G. Competitive Adsorption of Perfluoroalkyl Substances on Anion Exchange Resins in Simulated AFFF-Impacted Groundwater. *Chem. Eng. J.* **2018**, *348*, 494–502.

(30) Appleman, T. D.; Higgins, C. P.; Quiñones, O.; Vanderford, B. J.; Kolstad, C.; Zeigler-Holady, J. C.; Dickenson, E. R. V. Treatment of Poly- and Perfluoroalkyl Substances in U.S. Full-Scale Water Treatment Systems. *Water Res.* **2014**, *51*, 246–255.

(31) Deng, S.; Yu, Q.; Huang, J.; Yu, G. Removal of Perfluoroctane Sulfonate from Wastewater by Anion Exchange Resins: Effects of Resin Properties and Solution Chemistry. *Water Res.* **2010**, *44*, 5188–5195.

(32) Gao, Y.; Deng, S.; Du, Z.; Liu, K.; Yu, G. Adsorptive Removal of Emerging Polyfluoroalkyl Substances F-53B and PFOS by Anion-Exchange Resin: A Comparative Study. *J. Hazard. Mater.* **2017**, *323*, 550–557.

(33) Zaggia, A.; Conte, L.; Falletti, L.; Fant, M.; Chiorboli, A. Use of Strong Anion Exchange Resins for the Removal of Perfluoroalkylated Substances from Contaminated Drinking Water in Batch and Continuous Pilot Plants. *Water Res.* **2016**, *91*, 137–146.

(34) Alsbaiee, A.; Smith, B. J.; Xiao, L.; Ling, Y.; Helbling, D. E.; Dichtel, W. R. Rapid Removal of Organic Micropollutants from Water by a Porous  $\beta$ -Cyclodextrin Polymer. *Nature* **2016**, *529*, 190–194.

(35) Ling, Y.; Klemes, M. J.; Xiao, L.; Alsbaiee, A.; Dichtel, W. R.; Helbling, D. E. Benchmarking Micropollutant Removal by Activated Carbon and Porous  $\beta$ -Cyclodextrin Polymers under Environmentally Relevant Scenarios. *Environ. Sci. Technol.* **2017**, *51*, 7590–7598.

(36) Xiao, L.; Ling, Y.; Alsbaiee, A.; Li, C.; Helbling, D. E.; Dichtel, W. R.  $\beta$ -Cyclodextrin Polymer Network Sequesters Perfluoroctanoic Acid at Environmentally Relevant Concentrations. *J. Am. Chem. Soc.* **2017**, *139*, 7689–7692.

(37) Crini, G. Review: A History of Cyclodextrins. *Chem. Rev.* **2014**, *114*, 10940–10975.

(38) Xiao, L.; Ching, C.; Ling, Y.; Nasiri, M.; Klemes, M. J.; Reineke, T. M.; Helbling, D. E.; Dichtel, W. R. Cross-Linker Chemistry Determines the Uptake Potential of Perfluorinated Alkyl Substances by  $\beta$ -Cyclodextrin Polymers. *Macromolecules* **2019**, *52*, 3747–3752.

(39) Klemes, M. J.; Ling, Y.; Ching, C.; Wu, C.; Xiao, L.; Helbling, D. E.; Dichtel, W. R. Reduction of a Tetrafluoroterephthalonitrile- $\beta$ -Cyclodextrin Polymer to Remove Anionic Micropollutants and Perfluorinated Alkyl Substances from Water. *Angew. Chem., Int. Ed.* **2019**, *58*, 12049–12053.

(40) Ling, Y.; Klemes, M. J.; Steinschneider, S.; Dichtel, W. R.; Helbling, D. E. QSARs to Predict Adsorption Affinity of Organic Micropollutants for Activated Carbon and  $\beta$ -Cyclodextrin Polymer Adsorbents. *Water Res.* **2019**, *154*, 217–226.

(41) Li, C.; Klemes, M. J.; Dichtel, W. R.; Helbling, D. E. Tetrafluoroterephthalonitrile-Crosslinked  $\beta$ -Cyclodextrin Polymers for Efficient Extraction and Recovery of Organic Micropollutants from Water. *J. Chromatogr. A* **2018**, *1541*, 52–56.

(42) Ling, Y.; Alzate-Sánchez, D. M.; Klemes, M. J.; Dichtel, W. R.; Helbling, D. E. Evaluating the Effects of Water Matrix Constituents on Micropollutant Removal by Activated Carbon and  $\beta$ -Cyclodextrin Polymer Adsorbents. *Water Res.* **2020**, *173*, 115551.

(43) Wu, C.; Klemes, M. J.; Trang, B.; Dichtel, W. R.; Helbling, D. E. Exploring the Factors That Influence the Adsorption of Anionic PFAS on Conventional and Emerging Adsorbents in Aquatic Matrices. *Water Res.* **2020**, *182*, 115950.

(44) Weiss-Errico, M. J.; O'Shea, K. E. Detailed NMR Investigation of Cyclodextrin-Perfluorinated Surfactant Interactions in Aqueous Media. *J. Hazard. Mater.* **2017**, *329*, 57–65.

(45) Weiss-Errico, M. J.; Ghiviriga, I.; O'Shea, K. E. 19F NMR Characterization of the Encapsulation of Emerging Perfluoroether-carboxylic Acids by Cyclodextrins. *J. Phys. Chem. B* **2017**, *121*, 8359–8366.

(46) Palepu, R.; Reinsborough, V. C. Solution Inclusion Complexes of Cyclodextrins with Sodium Perfluoroctanoate. *Can. J. Chem.* **1989**, *67*, 1550–1553.

(47) Karoyo, A. H.; Borisov, A. S.; Wilson, L. D.; Hazendonk, P. Formation of Host-Guest Complexes of  $\beta$ -Cyclodextrin and Perfluoroctanoic Acid. *J. Phys. Chem. B* **2011**, *115*, 9511–9527.

(48) Place, B. J.; Field, J. A. Identification of Novel Fluorochemicals in Aqueous Film-Forming Foams Used by the US Military. *Environ. Sci. Technol.* **2012**, *46*, 7120–7127.

(49) Marvin; ChemAxon, 2018.

(50) Zhi, Y.; Liu, J. Sorption and Desorption of Anionic, Cationic and Zwitterionic Polyfluoroalkyl Substances by Soil Organic Matter and Pyrogenic Carbonaceous Materials. *Chem. Eng. J.* **2018**, *346*, 682–691.

(51) Wellington Laboratories. *New Products: Aqueous Film Forming Foam PFAS*, 2018.

(52) Ahrens, L.; Harner, T.; Shoeib, M.; Lane, D. A.; Murphy, J. G. Improved Characterization of Gas–Particle Partitioning for Per- and Polyfluoroalkyl Substances in the Atmosphere Using Annular Diffusion Denuder Samplers. *Environ. Sci. Technol.* **2012**, *46*, 7199–7206.

(53) Purolite. *Product Data Sheet: Purofine PFA694E*, 2020.

(54) Purolite. *Product Data Sheet: Purofine PFC100E*, 2020.

(55) Ji, W.; Xiao, L.; Ling, Y.; Ching, C.; Matsumoto, M.; Bisbey, R. P.; Helbling, D. E.; Dichtel, W. R. Removal of GenX and Perfluorinated Alkyl Substances from Water by Amine-Functionalized Covalent Organic Frameworks. *J. Am. Chem. Soc.* **2018**, *140*, 12677–12681.

(56) Deng, S.; Zhang, Q.; Nie, Y.; Wei, H.; Wang, B.; Huang, J.; Yu, G.; Xing, B. Sorption Mechanisms of Perfluorinated Compounds on Carbon Nanotubes. *Environ. Pollut.* **2012**, *168*, 138–144.

(57) Xiao, X.; Ulrich, B. A.; Chen, B.; Higgins, C. P. Sorption of Poly- and Perfluoroalkyl Substances (PFASs) Relevant to Aqueous Film-Forming Foam (AFFF)-Impacted Groundwater by Biochars and Activated Carbon. *Environ. Sci. Technol.* **2017**, *51*, 6342–6351.

(58) Dixit, F.; Barbeau, B.; Mostafavi, S. G.; Mohseni, M. Efficient Removal of GenX (HFPO-DA) and Other Perfluorinated Ether Acids from Drinking and Recycled Waters Using Anion Exchange Resins. *J. Hazard. Mater.* **2020**, *384*, 121261.

(59) Schaefer, C. E.; Nguyen, D.; Ho, P.; Im, J.; LeBlanc, A. Assessing Rapid Small-Scale Column Tests for Treatment of Perfluoroalkyl Acids by Anion Exchange Resin. *Ind. Eng. Chem. Res.* **2019**, *58*, 9701–9706.

(60) Gremmel, C.; Frömel, T.; Knepper, T. P. HPLC-MS/MS Methods for the Determination of 52 Perfluoroalkyl and Polyfluoroalkyl Substances in Aqueous Samples. *Anal. Bioanal. Chem.* **2017**, *409*, 1643–1655.

(61) Schaefer, C. E.; Culina, V.; Nguyen, D.; Field, J. Uptake of Poly- and Perfluoroalkyl Substances at the Air–Water Interface. *Environ. Sci. Technol.* **2019**, *53*, 12442–12448.

(62) Yu, Q.; Zhang, R.; Deng, S.; Huang, J.; Yu, G. Sorption of Perfluorooctane Sulfonate and Perfluorooctanoate on Activated Carbons and Resin: Kinetic and Isotherm Study. *Water Res.* **2009**, *43*, 1150–1158.

(63) Zhou, Q.; Deng, S.; Zhang, Q.; Fan, Q.; Huang, J.; Yu, G. Sorption of Perfluorooctane Sulfonate and Perfluorooctanoate on Activated Sludge. *Chemosphere* **2010**, *81*, 453–458.

(64) Park, M.; Wu, S.; Lopez, I. J.; Chang, J. Y.; Karanfil, T.; Snyder, S. A. Adsorption of Perfluoroalkyl Substances (PFAS) in Groundwater by Granular Activated Carbons: Roles of Hydrophobicity of PFAS and Carbon Characteristics. *Water Res.* **2020**, *170*, 115364.

(65) Luehrs, D. C.; Hickey, J. P.; Nilsen, P. E.; Godbole, K. A.; Rogers, T. N. Linear Solvation Energy Relationship of the Limiting Partition Coefficient of Organic Solutes between Water and Activated Carbon. *Environ. Sci. Technol.* **1996**, *30*, 143–152.

(66) Apul, O. G.; Wang, Q.; Shao, T.; Rieck, J. R.; Karanfil, T. Predictive Model Development for Adsorption of Aromatic Contaminants by Multi-Walled Carbon Nanotubes. *Environ. Sci. Technol.* **2013**, *47*, 2295–2303.

(67) Munoz, G.; Ray, P.; Mejia-Avendaño, S.; Vo Duy, S.; Tien Do, D.; Liu, J.; Sauvé, S. Optimization of Extraction Methods for Comprehensive Profiling of Perfluoroalkyl and Polyfluoroalkyl Substances in Fire Fighting Foam Impacted Soils. *Anal. Chim. Acta* **2018**, *1034*, 74–84.

(68) Barzen-Hanson, K. A.; Davis, S. E.; Kleber, M.; Field, J. A. Sorption of Fluorotelomer Sulfonates, Fluorotelomer Sulfonamido Betaines, and a Fluorotelomer Sulfonamido Amine in National Foam Aqueous Film-Forming Foam to Soil. *Environ. Sci. Technol.* **2017**, *51*, 12394–12404.

(69) Nickerson, A.; Maizel, A. C.; Kulkarni, P. R.; Adamson, D. T.; Kornuc, J. J.; Higgins, C. P. Enhanced Extraction of AFFF-Associated PFASs from Source Zone Soils. *Environ. Sci. Technol.* **2020**, *54*, 4952–4962.

(70) Mejia-Avendaño, S.; Munoz, G.; Sauvé, S.; Liu, J. Assessment of the Influence of Soil Characteristics and Hydrocarbon Fuel Cocontamination on the Solvent Extraction of Perfluoroalkyl and Polyfluoroalkyl Substances. *Anal. Chem.* **2017**, *89*, 2539–2546.

(71) Klemes, M. J.; Ling, Y.; Chiapasco, M.; Alsbaei, A.; Helbling, D. E.; Dichtel, W. R. Phenolation of Cyclodextrin Polymers Controls Their Lead and Organic Micropollutant Adsorption. *Chem. Sci.* **2018**, *9*, 8883–8889.

(72) Wang, W.; Mi, X.; Zhou, Z.; Zhou, S.; Li, C.; Hu, X.; Qi, D.; Deng, S. Novel Insights into the Competitive Adsorption Behavior and Mechanism of Per- and Polyfluoroalkyl Substances on the Anion-Exchange Resin. *J. Colloid Interface Sci.* **2019**, *557*, 655–663.